

Lindane suppresses the lipid-bilayer permeability in the main transition region

Mads C. Sabra, Kent Jørgensen, Ole G. Mouritsen *

Department of Physical Chemistry, The Technical University of Denmark, Building 206, DK-2800 Lyngby, Denmark

Received 19 December 1995; revised 14 February 1996; accepted 15 February 1996

Abstract

The effects of a small molecule, the insecticide lindane, on unilamellar DMPC bilayers in the phase transition region, have been studied by means of differential scanning calorimetry and fluorescence spectroscopy. The calorimetric data show that increasing concentrations of lindane broaden the transition and lower the transition temperature, without changing the transition enthalpy significantly. Lindane therefore enhances the thermal fluctuations of the bilayer. The calorimetric data furthermore suggest that the bilayer structure is intact and not disrupted by even high concentrations (32 mol%) of lindane. Fluorescence spectroscopy was used to measure the passive permeability of unilamellar DMPC bilayers to Co^{2+} ions. The data show that lindane seals the bilayer for Co^{2+} penetration and that this effect increases with increasing lindane concentration. The results are discussed in relation to the effects on the permeability of other small molecules, e.g., anesthetics.

Keywords: Lindane; Lipid bilayer; Permeability; Phase transition; Fluorescence spectroscopy

1. Introduction

It is widely accepted that the toxicity of hydrocarbons is, at least partly, due to their accumulation in the non-polar core of the lipid-bilayer component of biological membranes [1]. It remains, however, unclear whether the toxic effects of hydrocarbons are due to specific interactions with protein receptors, or whether the hydrocarbons modify the lipid bilayer structure of the membranes by more non-specific interactions which in turn cause the toxicity, e.g., by a change in the lipid environment around the membrane proteins or by a change in the properties of the bilayer itself, e.g., the passive ion permeability.

Insecticides are usually small hydrocarbon compounds of a considerable hydrophobicity. Important examples include parathion, malathion, DDT and lindane. Most of the studies of the physico-chemical effects of these insecticides on lipid membranes have been performed on multi-

lamellar lipid vesicles, whereas virtually no literature exists on interactions with unilamellar vesicles, which more faithfully resemble biological membranes. A common focus of these studies, e.g., for lindane [2–10], has been to elucidate the action of the insecticides on the lipid bilayer structure considering the insecticide as a small molecule which is dissolved in the hydrophobic lipid core of the membrane. In the present paper, we use unilamellar vesicles to study the effects of lindane on the thermal properties and on the passive bilayer permeability of DMPC bilayers in the region of the main phase transition. The chemical structure of lindane is shown in the inset of Fig. 1.

To measure the passive permeability of the bilayers, we use unilamellar vesicles labeled with the fluorescent probe NBD-PE (a headgroup labeled lipid analog) on the outer and inner bilayer leaflets. Addition of the quencher Co^{2+} to the aqueous phase results in an immediate reduction of the fluorescence from the outer surfaces. The subsequent decrease of the fluorescence from the inner surfaces is a measure of the ability of Co^{2+} to penetrate the bilayer, i.e., a measure of the passive permeability. This method of probing the bilayer permeability is a modification of a method originally proposed by Langner and Hui [11].

Abbreviations: DMPC, dimyristoylphosphatidylcholine; DSC, differential scanning calorimetry; NBD-PE, *N*-(7-nitrobenz-2-oxa-1,3-diazol-4-yl)phosphatidylethanolamine; lindane, γ -1,2,3,4,5,6-hexachlorocyclohexane.

* Corresponding author. Fax: +45 45934808; e-mail: ogm@fki.dtu.dk.

In the literature, two models have been proposed for the mechanism of penetration of small ions through lipid bilayers in the transition region [12]. One is the model of Doniach [13], which assumes that the energy barrier for permeability is directly related to the lateral compressibility of the bilayer, i.e., to the intensity of the density fluctuations. The density fluctuations imply dynamic lateral bilayer heterogeneity in terms of formation of lipid domains and associated interfacial regions [14]. The other model, which is a microscopic model, assumes that the permeability is high through interfacial regions between gel and fluid domains formed in the transition region, and low through the bulk gel and fluid phases [15,16].

The simple models for the passive permeability outlined above could be extended to include the effects of small molecules simply by calculating the effects of these molecules on the lateral density fluctuations or on the amount of interface, respectively. However, in this paper we shall present arguments based on experimental data, suggesting that the passive permeability as affected by small molecules has a more complex behavior than the simple extended models allow for, and that the permeability of ions as affected by small molecules may be related to details of the physico-chemical and structural properties of these molecules.

2. Materials and methods

2.1. Chemicals

DMPC at least 99% pure was obtained from Avanti Polar Lipids (Birmingham, AL) and used for most of the experiments described in this paper. DMPC for the particular DSC experiments shown in Fig. 1 was obtained from Sigma (St. Louis, MO) and had a purity of at least 98%. $\text{CoCl}_2 \cdot 6\text{H}_2\text{O}$ was purchased from Aldrich (Steinheim, Germany). Lindane of commercial grade was obtained from Sigma. NBD-PE was purchased from Molecular Probes (Eugene, OR). All chemicals were used without further purification.

2.2. Preparation of vesicles

To produce NBD-PE labeled multilamellar vesicles of DMPC, the dry lipid and NBD-PE were co-solubilized in chloroform. The chloroform was driven off by a stream of nitrogen, and the samples were stored under vacuum for at least 12 h. The resulting dry lipid/NBD-PE mixtures were then suspended in a KCl solution consisting of 50 mM KCl and 1 mM NaN_3 . The temperature was kept at 40°C for at least 1 h and during this period the suspensions were shaken vigorously several times. To produce unilamellar vesicles, the suspensions of multilamellar vesicles were extruded ten times through two stacked 100 nm pore filters using a hydrostatic pressure of 30 atm [17,18]. The final

lipid concentrations in the stock suspensions were about 3.5 mM, and the NBD-PE concentration was 1% of lipid.

Two different methods were used to include lindane in the lipid systems. For the lowest concentration of lindane, the stock unilamellar vesicles were diluted in the KCl solution saturated with lindane. This gives a total concentration of lindane in the system of 25–50 μM [10]. To obtain higher concentrations of lindane it was necessary to co-solubilize the lindane with the lipid in chloroform prior to suspending the mixture in KCl solution saturated with lindane and prior to extrusion. The quoted lindane molar concentrations were calculated on the basis of the total lipid and lindane concentrations before extrusion. This only provides an estimate of the lindane content, since a fraction of the total lipid and lindane content is lost during the extrusion procedure.

2.3. Differential scanning calorimetry

Differential scanning calorimetry was used to measure the excess heat capacity, C_p , and was performed using an MC-2 Ultrasensitive Scanning Calorimeter from Microcal (Northampton, MA, USA). The calorimeter is of the power-compensating type with cell volumes of 1.2 ml. During scanning the reference cell contained KCl solution. The samples were subject to a hydrostatic pressure of 2.5 atm (absolute) during scanning.

2.4. Fluorescence measurements

Fluorescence-emission time-traces were recorded using a DMX 1100 Spectrofluorometer from SLM-Aminco (Urbana, IL, USA). Excitation and emission wavelengths were 465 nm and 535 nm, respectively. Excitation and emission slits were 2 nm and 4 nm, respectively. The temperature of the sample was measured and recorded continuously during the experiments using an internal temperature probe placed in the sample cuvette. The temperature was maintained using a circulating water bath. The thermostated cuvette holder allowed the temperature to be controlled to a precision of approximately $\pm 0.1^\circ\text{C}$.

Samples for fluorescence studies were prepared by diluting the suspension of unilamellar vesicles in KCl solution. The lindane-containing systems were diluted in a saturated lindane solution. The final concentrations were 70 μM in lipid. Each sample was allowed to equilibrate for at least 1 h at the relevant temperature before loading it into the fluorometer, which was thermostated to the relevant temperature. Each sample consisted of 3.0 ml lipid suspension.

After 100 s of constant temperature and fluorescence intensity, 150 μl of a 0.2 M CoCl_2 stock solution were added. The resulting Co^{2+} concentration was 9.5 mM. The decay of fluorescence intensity after addition of Co^{2+} was recorded over a period of 500 s.

2.5. Data analysis

Baselines in the form of constants were subtracted from the C_p curves, i.e., a constant was subtracted from each of the curves before integration and determination of the peak position, T_m , and the peak width at half maximum, $T_{1/2}$. This constant was chosen such that the excess heat capacity was zero at $T = 35^\circ\text{C}$. The integration also gives the sum of the transition enthalpy and the enthalpy usually hidden in the wings of the transition. This is commented on later. The fluorescence-intensity time-traces were normalized to the ratio of fluorescence before Co^{2+} treatment to obtain the relative fluorescence intensity after addition of Co^{2+} . It was taken into account that the sample was diluted by addition of Co^{2+} solution. Fitting of the decays was performed using the least-squares method with Microcal Origin™ software.

3. Results

3.1. Differential scanning calorimetry

Differential scanning calorimetry was applied to unlabeled DMPC unilamellar vesicles containing 0 mol%, 6 mol%, 11 mol%, 20 mol% and 27 mol% lindane. The results for C_p are shown in Fig. 1. It is clear that lindane causes the main transition to broaden and the midpoint of the transition to be shifted towards lower temperatures. Both of these effects increase progressively with the lindane concentration, as can be seen from Fig. 2a and 2b. Fig. 2a shows the main transition temperature, defined by the peak position T_m , as a function of the lindane concentration. It appears that T_m is linearly dependent on the lindane concentration. In Fig. 2b, the width of the transition is shown as measured by the peak width at half maximum. The width is approximately linearly dependent on the lindane concentration.

The areas under the C_p curves shown in Fig. 1 were measured. These areas are denoted by ΔH . Baselines in the form of constants were subtracted from the curves. Hence, ΔH represents only an estimate of the transition enthalpy. More precisely, ΔH is the transition enthalpy plus the enthalpy in the wings of the transition (possibly including the pre-transition), and is therefore somewhat larger than the transition enthalpy. In the case of the system without lindane, we have tried to subtract a baseline as usual and then measured the area under the curve. This gives a value of approx. 6 kcal/mol for the transition enthalpy, which is in good agreement with the value of 6.5 kcal/mol obtained for multilamellar systems [19]. The variation of ΔH with the concentration of lindane is shown in Fig. 2c. ΔH seems to decrease slightly with increasing lindane concentration. However, Fig. 1 shows that a low-temperature wing of the transition extends below the scanned interval in the case of the lindane-con-

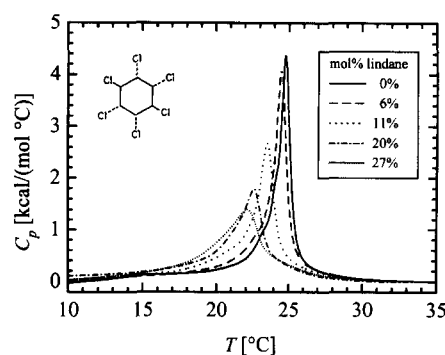


Fig. 1. Excess heat capacities of unilamellar vesicles of DMPC loaded with lindane. The curves were obtained by differential scanning calorimetry as up-scans at a scan-rate of $60^\circ\text{C}/\text{h}$. The lipid concentrations were 3.4 mM. The inset shows the chemical structure of lindane.

taining systems. Taking this into account, the apparent decrease of ΔH might not be significant. In any case, considering the large amounts of lindane in the bilayer, the effect of decreasing ΔH is small.

In order to relate some of the results for the permeability presented in the following section directly to the heat capacity, two DSC scans for unilamellar vesicles including the NBD-PE fluorescent probe were recorded as shown in Fig. 3. One of the curves is from a sample without lindane and the other is from a sample with a high (32 mol%) lindane content. These samples were taken from the stock suspensions also used for the fluorescence spectroscopy experiments. In the case of the system without lindane, there is a small shoulder on the low-temperature side of the peak. We shall return to a discussion of this shoulder in the following section. The midpoint of the transition is at 24.7°C for the system without lindane and at 20.9°C for the system with the high lindane content. These values are in agreement with the linear relationship indicated in Fig. 2a for unlabeled vesicles. The values for the widths at half peak height, 0.55°C in the case of the pure system and 3.7°C for the lindane-containing system, follow the linear relationship in Fig. 2b. The areas under the curves, 8.0 kcal/mol and 9.6 kcal/mol for the system with and without lindane, respectively, indicate a slight decrease of the transition enthalpy due to the presence of lindane. The values for the areas should not be directly compared with the values given in Fig. 2c, since the lipid concentrations in the two series of experiments might have differed. Within each series, however, the lipid concentration is expected not to vary significantly.

The C_p curves presented in Figs. 1 and 3 strongly suggest that even in the presence of large amounts of lindane, the bilayer structure is intact and not disrupted by lindane. Consecutive scans showed no change in the C_p curves. We shall in the following refer to the transition from the gel state to the fluid state as the main transition, even though it is likely that lateral phase separation occurs due to the high lindane content. The fact that the bilayer

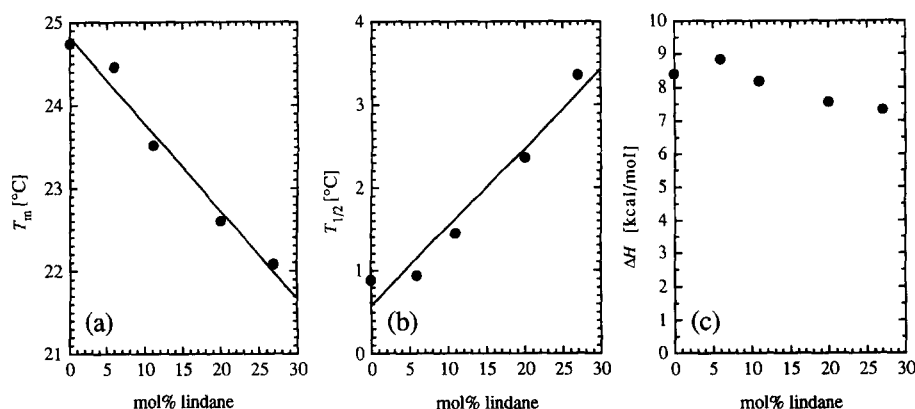


Fig. 2. Data extracted from the C_p curves shown in Fig. 1. The straight lines represent linear regression of the data. (a) Dependence of the transition temperature, T_m , on the lindane concentration for unilamellar DMPC vesicles, as determined from the position of the peaks. (b) Variation of the width, $T_{1/2}$, at half peak height, with the lindane concentration. (c) The area, ΔH , under the heat capacity curves as a function of the lindane concentration. ΔH represents only an estimate of the transition enthalpy, as described in the text.

structure is intact in the presence of lindane is also supported by the shape of the fluorescence time-traces, as will be discussed later.

3.2. Fluorescence spectroscopy

Co^{2+} is known to be an efficient reversible quencher of fluorescence from the NBD fluorescent group [20]. Furthermore, when attached to the headgroup of a lipid (as in NBD-PE) which is subsequently incorporated into a bilayer, the NBD moiety is expected to be located in the headgroup/water interfacial region and not in the hydrophobic core of the membrane [20]. Hence, addition of Co^{2+} to NBD-PE labeled unilamellar vesicles results immediately in the quenching of the fluorophores located on the outer leaflets of the vesicles. The rate of quenching the fluorophores located on the inner leaflets depends on the ability of the quencher to penetrate the bilayers. A high permeability of the bilayers results in a fast decay of the fluorescence intensity, whereas a low permeability results in a slow decay.

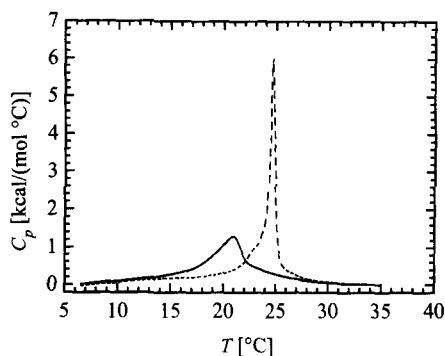


Fig. 3. Excess heat capacities of pure unilamellar DMPC vesicles labeled with 1 mol% NBD-PE. The C_p curves were obtained as up-scans at a scan-rate of 20 °C/h. The two curves correspond to a system without lindane (dashed line) and to a system containing 32 mol% lindane (solid line). The lipid concentrations were 3.6 mM.

In order to estimate the quenching constant, K_{SV} , defined by the Stern–Volmer equation [21],

$$\frac{F_0}{F} = 1 + K_{SV}[\text{Co}^{2+}] \quad (1)$$

where F_0 and F are the fluorescence intensities before and after the addition of the quencher, NBD-PE-labeled unilamellar DMPC vesicles were slowly cycled between 30 °C and 20 °C several times before the fluorescence intensities below ($T = 20$ °C), at ($T = 25$ °C) and above ($T = 30$ °C) the main transition were measured. Then (at $T = 25$ °C) 30 μl 1 M Co^{2+} were added and the cycling procedure repeated, before measuring the fluorescence intensities at 20 °C, 25 °C and 30 °C, now in the presence of 10 mM Co^{2+} . An estimate of the quenching constant was calculated according to Eq. (1), the result being $K_{SV} \approx 80 \text{ M}^{-1}$ at all three temperatures. Hence, we conclude that K_{SV} does not depend significantly on the physical state (gel, fluid or transitional) of the bilayer. A wide range of values for K_{SV} are quoted in the literature, e.g., 13.8 M^{-1} [22], 59 M^{-1} [20], and 36 M^{-1} [23] for NBD-PE in PC bilayers. The value we have determined above is consistent with the permeability measurements we present below.

Three different systems were studied. One without lindane, one prepared by diluting the stock unilamellar vesicle suspension in a saturated lindane solution, and one containing 32 mol% lindane. We shall refer to these systems as the pure system, the system with the low lindane content and the system with the high lindane content, respectively.

At this point it should be noted that, due to the large membrane/water partition coefficient of lindane, it is not possible to perform a DSC scan corresponding to the system with the low lindane content. This is due to the fact that the lipid concentration in a fluorescence experiment must be much lower than the sensitivity of our calorimeter allows for. Since lindane is added as a saturated solution, the lindane/lipid ratio is much higher in the fluorescence

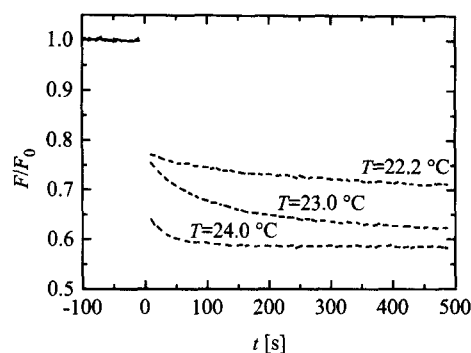


Fig. 4. Fluorescence-intensity time-traces obtained at $T = 22.2^\circ\text{C}$, $T = 23.0^\circ\text{C}$ and $T = 24.0^\circ\text{C}$ for systems without lindane. Co^{2+} was added at $t = 0$ s.

experiment than is feasible for a corresponding DSC experiment.

Figs. 4 and 5 show some examples of the fluorescence-intensity time-traces obtained by adding Co^{2+} to suspensions of NBD-PE labeled unilamellar DMPC vesicles with and without lindane. The gap (extending from -10 s to $+10$ s) in each of the time traces is due to our experimental setup, which did not allow for recording data while adding the quencher.

In Fig. 4 three time traces are shown for the system without lindane. The data were recorded at $T = 22.2^\circ\text{C}$, $T = 23.0^\circ\text{C}$ and $T = 24.0^\circ\text{C}$, respectively. In all three cases, there is an immediate reduction of the fluorescence intensity followed by a slower decay. This decay is slowest at $T = 22.2^\circ\text{C}$, faster at $T = 23.0^\circ\text{C}$, and at $T = 24.0^\circ\text{C}$ the decay is almost too fast to be recorded. This indicates that the penetration is slow below the transition, and fast at the transition. Near the transition, most of the decay takes place within the first 10 s after the addition of Co^{2+} , and is hence not recorded. For the slowest decay it is noticed that the immediate drop in intensity (corresponding to quenching of the outer leaflet) is a drop to about 78% of the original intensity. Using the quenching constant of 80

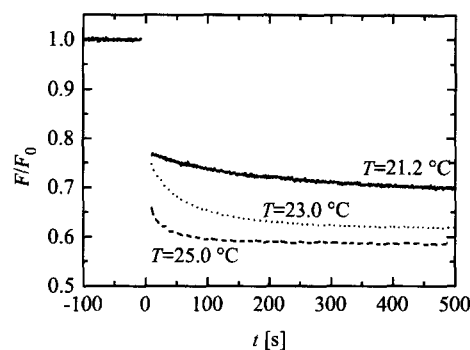


Fig. 5. Fluorescence-intensity time-traces obtained at $T = 21.2^\circ\text{C}$, $T = 23.0^\circ\text{C}$ and $T = 25.0^\circ\text{C}$ for a system with the high lindane content (solid line), a system with the low lindane content solution (dotted line) and for a system without lindane (dashed line), respectively. The data shown correspond to the fastest decay observed for each system. Co^{2+} was added at $t = 0$ s.

M^{-1} , we find that very close to 50% of the fluorophores are located on the outer leaflet, as expected.

Fig. 5 shows the fluorescence-intensity time-traces obtained at the temperature which resulted in the fastest decay for each of the three systems studied. The respective temperatures were $T = 25.0^\circ\text{C}$ for the system without lindane, $T = 23.0^\circ\text{C}$ for the system with the low lindane content and $T = 21.2^\circ\text{C}$ for the system with the high lindane content. These values are close to the peak positions in the corresponding DSC scans shown in Fig. 3. The time traces clearly demonstrate that the decay is fastest for the system without lindane and slowest for the system containing the most lindane. For the system without lindane it is noticed that already after about 200 s the fluorescence intensity has reached 59% of the original intensity; thereafter virtually no further decrease is observed, i.e., the penetration is complete. This is consistent with the estimated quenching constant, which predicts the intensity level at complete penetration to be 57% of the original intensity.

The decay of the fluorescence intensity does not follow single exponential kinetics. However, it is possible to fit the data to a sum of two exponentials, i.e., to a function of the form

$$x = A_1 e^{-k_1 t} + A_2 e^{-k_2 t} + x_0 \quad (2)$$

where x_0 is the level of the fluorescence at maximal quenching, i.e., $x_0 = 0.57$. We are not in a position to assign each of the individual time constants, k_1 and k_2 , to individual processes. Instead we define the 'average time constant', k_{av} , as

$$k_{av} = \frac{A_1 k_1 + A_2 k_2}{A_1 + A_2} \quad (3)$$

as proposed by Schwarz [24] to describe the overall characteristic time for a multi-exponential decay process. We

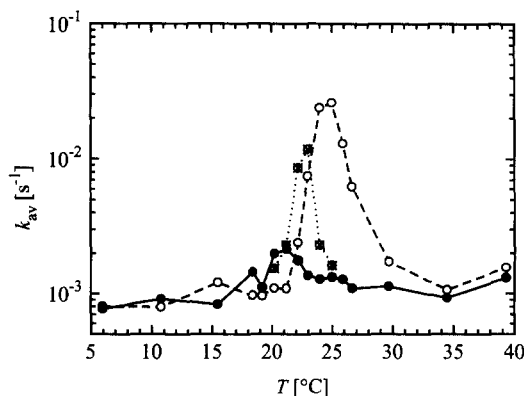


Fig. 6. The average time constant, k_{av} , for the penetration of Co^{2+} through unilamellar DMPC vesicles as a function of temperature. Each value plotted is an average over three experiments. Data are shown for a system without lindane (dashed line), a system with the low lindane content (dotted line) and for a DMPC system with the high lindane content (solid line).

shall use k_{av} as a measure of the characteristic time for Co^{2+} penetration through DMPC bilayers.

Fig. 6 shows the average time constant, k_{av} , for the decays. Each data point is an average over three experiments. For all three systems, there is a distinct peak at the main transition. In the case of the pure system and the system with the high lindane content, the peak correlates with the peak in the C_p curves, cf. Fig. 3. The peak corresponding to the system without lindane is more pronounced than the peak corresponding to the system with the low lindane content which in turn is more pronounced than the peak for the system with the high lindane content.

4. Discussion

We have presented the results from a combined calorimetric and fluorometric study of the effects of lindane on the permeability and on the transitional properties of unilamellar DMPC bilayers. This allows us to relate the bulk thermodynamic properties of the bilayers to the permeability, which might reflect the microscopic structural properties of the bilayer.

The lindane content in the membrane is not known with high precision, since partitioning between the lipid and the water phases is expected to occur and to vary with the temperature [6].

The results presented in Fig. 2a and 2b show, respectively, the systematic linear broadening and depression of the main transition of unilamellar DMPC vesicles as a function of the lindane content. The systematics in this behavior is similar to that found for multilamellar vesicles [10]. However, in unilamellar vesicles much larger concentrations of lindane are needed to produce an effect of comparable magnitude. A broadening and depression of the main transition have also been observed for other small molecules interacting with multilamellar lipid bilayers, e.g., the anesthetics halothane [25] and dibucaine [26].

The broadening of the transition reflects a disordering of the gel phase and, to a somewhat lesser extent, an ordering of the fluid phase, as found by Antunes-Madeira et al. by fluorescence polarization studies [7,8]. The lowering of T_m can be understood in terms of a freezing-point depression. From classical thermodynamics, however, a linear dependence of the freezing-point depression on the lindane concentration is expected to hold only for dilute solutions.

The estimated transition enthalpy seems to depend only slightly on the presence of lindane. This indicates that lindane takes up only a small excluded volume within the bilayer, i.e., lindane is intercalated between the acyl chains without hindering the acyl-chain movements.

Comparing the C_p curves for the two systems without lindane, cf. Figs. 1 and 3, it is clear that 1% NBD-PE does not influence the bilayer transitional properties significantly, the only difference being the size of the shoulder

on the low-temperature side of the transition. The origin of this shoulder is unclear, but it is not a result of the presence of NBD-PE, since it can also be detected in systems without NBD-PE, cf. Fig. 1. One possible explanation is that the samples contain residual multilamellar vesicles [27] or that the size distribution of the unilamellar vesicles is inhomogeneous.

In the following we shall assume that the average time constant, k_{av} , measured by fluorescence spectroscopy and shown in Fig. 6 can be used as a measure of the passive bilayer permeability. The experimental method that we use to measure the permeability has a few drawbacks which we shall mention shortly. Firstly, there might be complications due to the adsorption of Co^{2+} to the membrane surface, as reported by [20]. Furthermore, we do not know for sure that lindane does not influence the distribution of fluorophores between the outer and inner membrane leaflet, although our data suggest that this is not the case to any significant degree. However, neither of these drawbacks can interfere with the general trend of our results which display a number of features showing that the method used is capable of estimating the permeability of lipid membranes.

Several authors have observed a peak in the ion permeability of pure lipid bilayers at the main transition [12,28,29]. It has been proposed that this peak is due to packing defects at the interfaces occurring between gel and fluid domains formed as the bilayer undergoes the transition. Computer simulations on microscopic models support this hypothesis [16,30].

Computer simulations also indicate that the addition of small molecules (impurities), such as anesthetics, increase the amount of interface in a broad range around the transition [30,31]. This is believed to hold also for other small molecules like insecticides, specifically lindane [32].

It has been reported that in a DMPC/DPPC mixture, the permeability of small polar molecules exhibits a maximum when the fluid and gel domains coexist [33]. If addition of lindane leads to phase coexistence in the phase transition region it could therefore be expected that the permeability would increase.

However, our results clearly show that the permeability at the main transition is reduced by lindane, and that this effect is concentration dependent. Hence, the simple relationship between the amount of interface and the permeability does not seem to hold here, as it does in the case of several anesthetics [30,34].

We have two possible explanations of these observations. One explanation is that the lindane molecules seal the interfaces, so that these become less permeable. Lindane is expected to accumulate in the interfaces as suggested by the peak in the partition coefficient observed by Antunes-Madeira et al. [6]. This explanation may seem somewhat labored, but it represents no inconsistency with the general understanding of the basis for the permeability of lipid bilayers. Such changes in the properties of the

interfaces by lindane would probably also have a considerable effect on the function of proteins in biological membranes.

The other explanation is that the permeability is directly correlated with the intensity of the density fluctuations, as proposed by Doniach [13]. Since the intensity of the density fluctuations correlates closely with the intensity of the thermal fluctuations, i.e., the heat capacity, we can compare the C_p curves directly with the permeability curves. The resemblance of the two types of measurements is obvious, suggesting that the Doniach model for permeability holds also for the effect of small molecules on lipid bilayers.

It has, however, been observed that a decrease of the fluctuations in the presence of the local anesthetic procaine is accompanied by an increase of the permeability to ions [30]. It could be inferred that since procaine is a charged molecule, it disturbs the headgroup region and facilitates permeation of ions. This reflects that the headgroup region is an important barrier for permeation. For *p*-di-*t*-butylbenzene and butylated hydroxytoluene, which are also small hydrophobic molecules, a decrease in the permeability to ions around the main transition has been observed too [35]. It has also been reported that the polar anesthetics, chloroform and hexanol, decrease the activation energy for permeation, whereas their apolar counterparts, carbon tetrachloride and hexane, have almost no effect [36]. Furthermore, the *trans/cis* isomerization of an azobenzene derivative incorporated into lipid bilayers is reported to increase the permeability by orders of magnitude [37].

Previous studies of the effect of small organic molecules on the permeability of lipid bilayers have often been carried out at a single temperature, which is a few degrees away from the main transition of the pure bilayer [38,39] and only a few studies cover a wide temperature range [30,35,34]. Our results also show a slight increase of the permeability a few degrees below the transition, which, however, only reflects the shift of T_m towards lower temperatures. Correcting for the freezing-point depression in the case of lindane, we conclude that lindane seals the bilayer for the penetration of Co^{2+} , and that this effect is increasing with the lindane concentration.

When compared with previous studies, the results presented in this paper show that the concept of 'small molecules' interacting with lipid bilayers is too simple when it comes to explaining permeability effects. One has to consider the individual molecular structure in detail when trying to predict its physico-chemical effects.

Acknowledgements

This work was supported by Brodrene Hartmanns Foundation via an equipment grant, by the Danish Natural Science Research Council (SNF) and by The Danish Tech-

nical Research Council (STVF). The authors are grateful to Prof. Rodney L. Biltonen for advice during preparation of the manuscript. The authors also thank Jens Pedersen for a thorough reading of the manuscript. O.G.M. is an Associate Fellow of the Canadian Institute for Advanced Research.

References

- [1] Sikkema, J., De Bont, J.A.M. and Poolman, B. (1995) *Microbiol. Rev.* 59, 201–222.
- [2] Lakowicz, J., Hogen, D. and Omann, G. (1977) *Biochim. Biophys. Acta* 471, 401–411.
- [3] Lakowicz, J.R. and Hogen, D. (1980) *Chem. Phys. Lipids* 26, 1–40.
- [4] Omann, G.M. and Lakowicz, J.R. (1982) *Biochim. Biophys. Acta* 684, 83–95.
- [5] Bach, D. and Sela, B.-A. (1984) *Biochem. Pharmacol.* 33, 2227–2230.
- [6] Antunes-Madeira, M.C. and Madeira, V.M.C. (1985) *Biochim. Biophys. Acta* 820, 165–172.
- [7] Antunes-Madeira, M.C. and Madeira, V.M.C. (1989) *Biochim. Biophys. Acta* 982, 161–166.
- [8] Antunes-Madeira, M.C., Almeida, L.M. and Madeira, V.M.C. (1990) *Biochim. Biophys. Acta* 1022, 110–114.
- [9] Verma, S.P. and Rastogi, A. (1990) *Biochim. Biophys. Acta* 1027, 59–64.
- [10] Sabra, M.C., Jørgensen, K. and Mouritsen, O.G. (1995) *Biochim. Biophys. Acta* 1233, 89–104.
- [11] Langner, M. and Hui, S.W. (1993) *Chem. Phys. Lipids* 65, 23–30.
- [12] Mouritsen, O.G., Jørgensen, K. and Hønger, T. (1995) in *Permeability and Stability of Lipid Bilayers* (Disalvo, E.A. and Simon, S.A., eds.), pp. 137–160, CRC Press, Boca Raton, FL.
- [13] Doniach, S. (1978) *J. Chem. Phys.* 68, 4912–4916.
- [14] Mouritsen, O.G. and Jørgensen, K. (1994) *Chem. Phys. Lipids* 73, 3–25.
- [15] Kanehisa, M.I. and Tsong, T.Y. (1978) *J. Am. Chem. Soc.* 100, 424–432.
- [16] Cruzeiro-Hansson, L. and Mouritsen, O.G. (1988) *Biochim. Biophys. Acta* 944, 63–72.
- [17] Hope, M.J., Bally, M.B., Webb, G. and Cullis, P.R. (1985) *Biochim. Biophys. Acta* 812, 55–65.
- [18] Mayer, L.D., Hope, M.J. and Cullis, P.R. (1986) *Biochim. Biophys. Acta* 858, 161–168.
- [19] Lasic, D. (1993) *Liposomes: From Physics to Applications*, Elsevier Science, Amsterdam.
- [20] Homan, R. and Eisenberg, M. (1985) *Biochim. Biophys. Acta* 812, 485–492.
- [21] Lakowicz, J.R. (1983) *Principles of Fluorescence Spectroscopy*, Plenum Press, New York.
- [22] Morris, S.J., Bradley, D. and Blumenthal, R. (1985) *Biochim. Biophys. Acta* 818, 365–372.
- [23] Chattopadhyay, A. and London, E. (1988) *Biochim. Biophys. Acta* 938, 24–34.
- [24] Schwarz, G. (1965) *J. Mol. Biol.* 11, 64–77.
- [25] Mountcastle, D.B., Biltonen, R.L. and Halsey, M.J. (1978) *Proc. Natl. Acad. Sci. USA* 75, 4906–4910.
- [26] Van Osdol, W.W., Ye, Q., Johnson, M.L. and Biltonen, R.L. (1992) *Biophys. J.* 63, 1011–1017.
- [27] Nagamo, H., Yao, H. and Ema, K. (1995) *Phys. Rev. E* 51, 3363–3367.
- [28] Papahadjopoulos, D., Jacobson, K. and Isac, T. (1973) *Biochim. Biophys. Acta* 311, 330–348.
- [29] Georgallas, A., MacArthur, J.D., Ma, X.-P., Nguyen, C.V., Palmer, G.R., Singer, M.A. and Tse, M.Y. (1987) *J. Chem. Phys.* 86, 7218–7226.

- [30] Tsong, T.Y., Greenberg, M. and Kanehisa, M.I. (1977) *Biochemistry* 16, 3115–3121.
- [31] Jørgensen, K., Ipsen, J.H., Mouritsen, O.G. and Zuckermann, M.J. (1993) *Chem. Phys. Lipids* 65, 205–216.
- [32] Jørgensen, K., Ipsen, J.H., Mouritsen, O.G., Bennett, D. and Zuckermann, M.J. (1991) *Biochim. Biophys. Acta* 1067, 241–253.
- [33] Clerc, S.G. and Thompson, T.E. (1995) *Biophys. J.* 68, 2333–2341.
- [34] Singer, M.A. and Jain, M.K. (1980) *Can. J. Biochem.* 58, 815–821.
- [35] Singer, M. (1979) *Chem. Phys. Lipids* 25, 15–28.
- [36] Inoue, T., Kamaya, H. and Ueda, I. (1985) *Biochim. Biophys. Acta* 812, 393–401.
- [37] Tanaka, M., Sato, T. and Yonezawa, Y. (1995) *Langmuir* 11, 2834–2836.
- [38] Johnson, S.M., Miller, K.W. and Bangham, A.D. (1973) *Biochim. Biophys. Acta* 307, 42–57.
- [39] Barchfeld, G.L. and Deamer, D.W. (1988) *Biochim. Biophys. Acta* 944, 40–48.